

Electronic Supplementary Information

In-Situ Growth of Perovskite Stacking Layer for High Efficiency Carbon-Based Hole Conductor Free Perovskite Solar Cells

Jianhua Liu,^a Qisen Zhou,^a Nan Kyi Kyi Thein,^{b,c} Lei Tian,^b Donglin Jia,^a Erik M. J. Johansson,^b and Xiaoliang Zhang^{a}*

a. School of Materials Science and Engineering, Beihang University, 100191 Beijing, China.

*Email: xiaoliang.zhang@buaa.edu.cn

b. Department of Chemistry-Ångström, Physical Chemistry, Uppsala University, 75120 Uppsala, Sweden.

c. Department of Physics-Materials Science Research Laboratory, Mandalay University, Mandalay, Myanmar.

Content

Figures:

Fig. S1: XRD patterns of perovskite film before and after the IPA treatment.

Fig. S2: Tauc plot of MAPbI₃ perovskite and MAPbI₃/MAPbI_xBr_{3-x}-PSS from the light absorbance spectra.

Fig. S3: Overview XPS spectra of MAPbI₃ perovskite and MAPbI₃/MAPbI_xBr_{3-x}-PSS.

Fig. S4: Time of Flight Secondary Ion Mass Spectrometry of the Br element in the MAPbI₃/MAPbI_xBr_{3-x}-PSS.

Fig. S5. Statistic of the MAPbI₃-based PSC and MAPbI₃/MAPbI_xBr_{3-x}-based PSC.

Fig. S6. Photovoltaic performance of the MAPbI₃-based PSC with Spiro-OMeTAD and P3HT as the HTM

Fig. S7: Integrated photocurrent from the IPCE spectra.

Fig. S8: MPP tracking of the photocurrent density and photovoltage of the MAPbI₃/MAPbI_xBr_{3-x}-based PSC.

Fig. S9: Normalized PL spectra of the MAPbI₃ perovskite and MAPbI₃/MAPbI_xBr_{3-x}-PSS prepared on the microscopy slide.

Fig. S10. Electron lifetime as function of V_{oc} in the MAPbI₃ perovskite and MAPbI₃/MAPbI_xBr_{3-x}-PSS solar cells.

Fig. S11: Nyquist plots and their fitting curves of the MAPbI₃-based and MAPbI₃/MAPbI_xBr_{3-x}-based PSC.

Tables:

Table S1. Fitted parameters of the PL decay of MAPbI₃ perovskite and MAPbI₃/MAPbI_xBr_{3-x}-PSS.

Table S2. Summarized photovoltaic performance of the carbon electrode-based HTM-free PSCs.

Table S3. Summarized photovoltaic performance of the carbon electrode-based PSCs with HTM in the device.

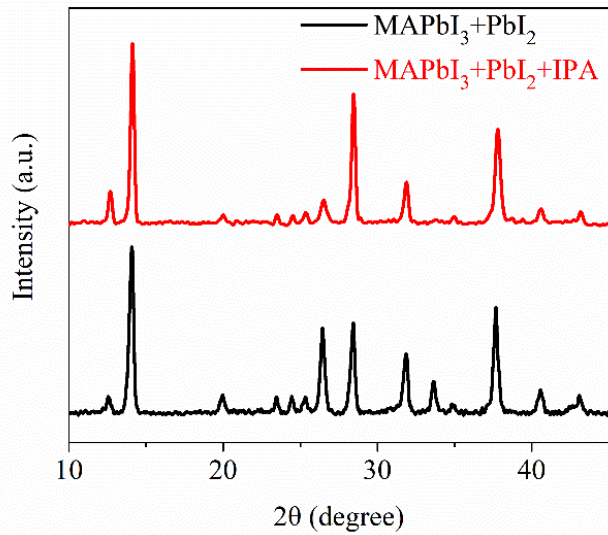


Fig. S1. XRD pattern of the perovskite layer ($\text{MAPbI}_3 + \text{PbI}_2$) before and after the IPA treatment. The perovskite layer was prepared on the FTO/c-TiO₂/m-TiO₂ substrates. The improved peak intensity of the PbI_2 at the $\sim 12.7^\circ$ may due to that the MA was washed away by IPA and then more PbI_2 left on the sample.

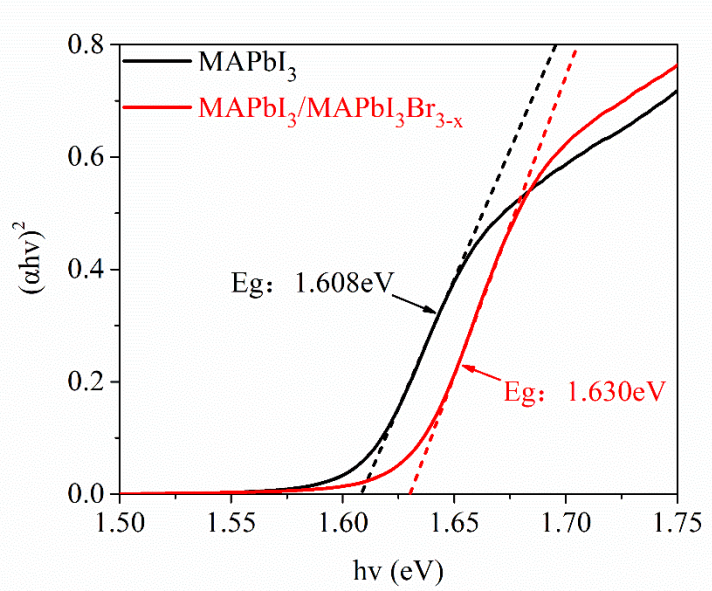


Fig. S2. Tauc plot of the MAPbI_3 perovskite and $\text{MAPbI}_3/\text{MAPbI}_x\text{Br}_{3-x}\text{-PSS}$.

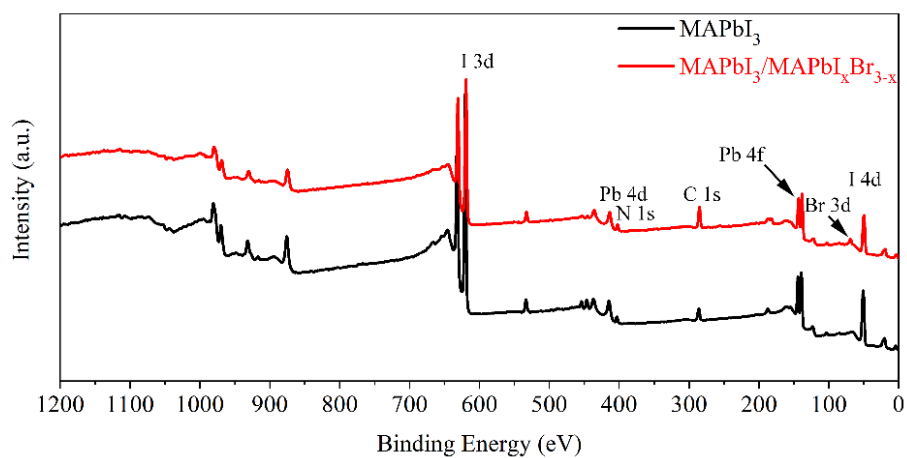


Fig. S3. Overview XPS spectra of the MAPbI_3 perovskite and $\text{MAPbI}_3/\text{MAPbI}_x\text{Br}_{3-x}\text{-PSS}$.

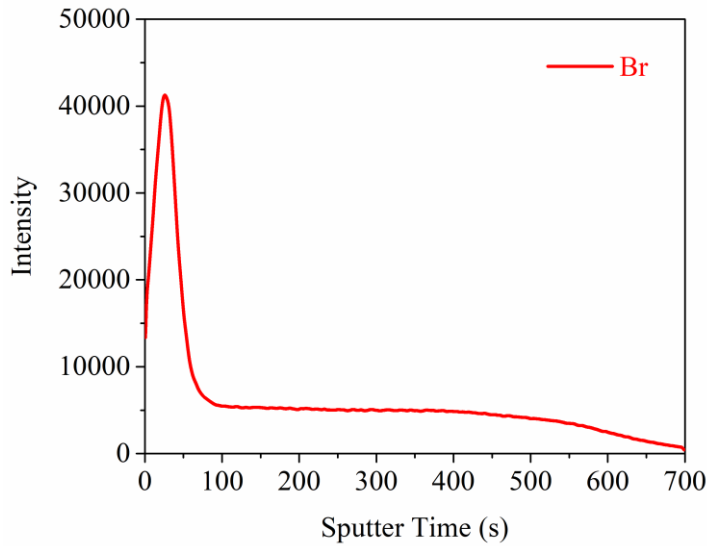


Fig. S4. Time of flight secondary ion mass spectrometry of the Br element in the $\text{MAPbI}_3/\text{MAPbI}_x\text{Br}_{3-x}$ -PSS. Sputtering speed is about 1 nm/s. The Br element is mainly distributing at the top part of $\text{MAPbI}_3/\text{MAPbI}_x\text{Br}_{3-x}$ -PSS film with a depth of ~ 75 nm, which suggests that the $\text{MAPbI}_x\text{Br}_{3-x}$ has a thickness of ~ 75 nm.

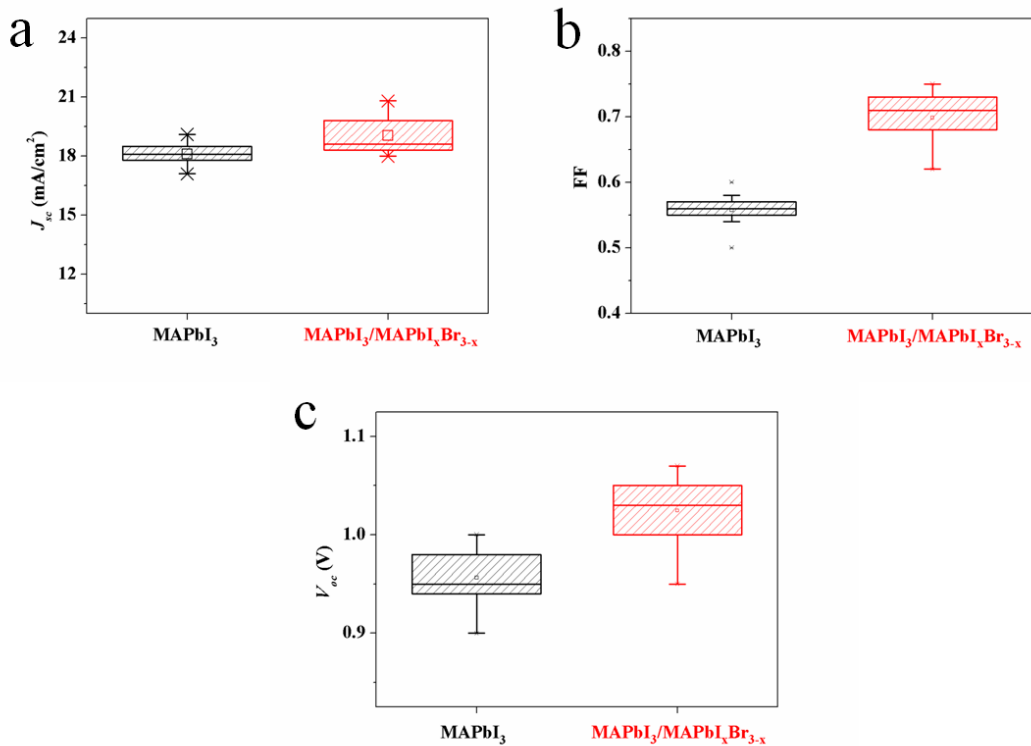


Fig. S5. Statistic of the (c) J_{sc} , (d) FF, and V_{oc} and of the MAPbI_3 -based PSC and (e) $\text{MAPbI}_3/\text{MAPbI}_x\text{Br}_{3-x}$ -based PSC. 16 solar cell devices from different branches were used for stastic.

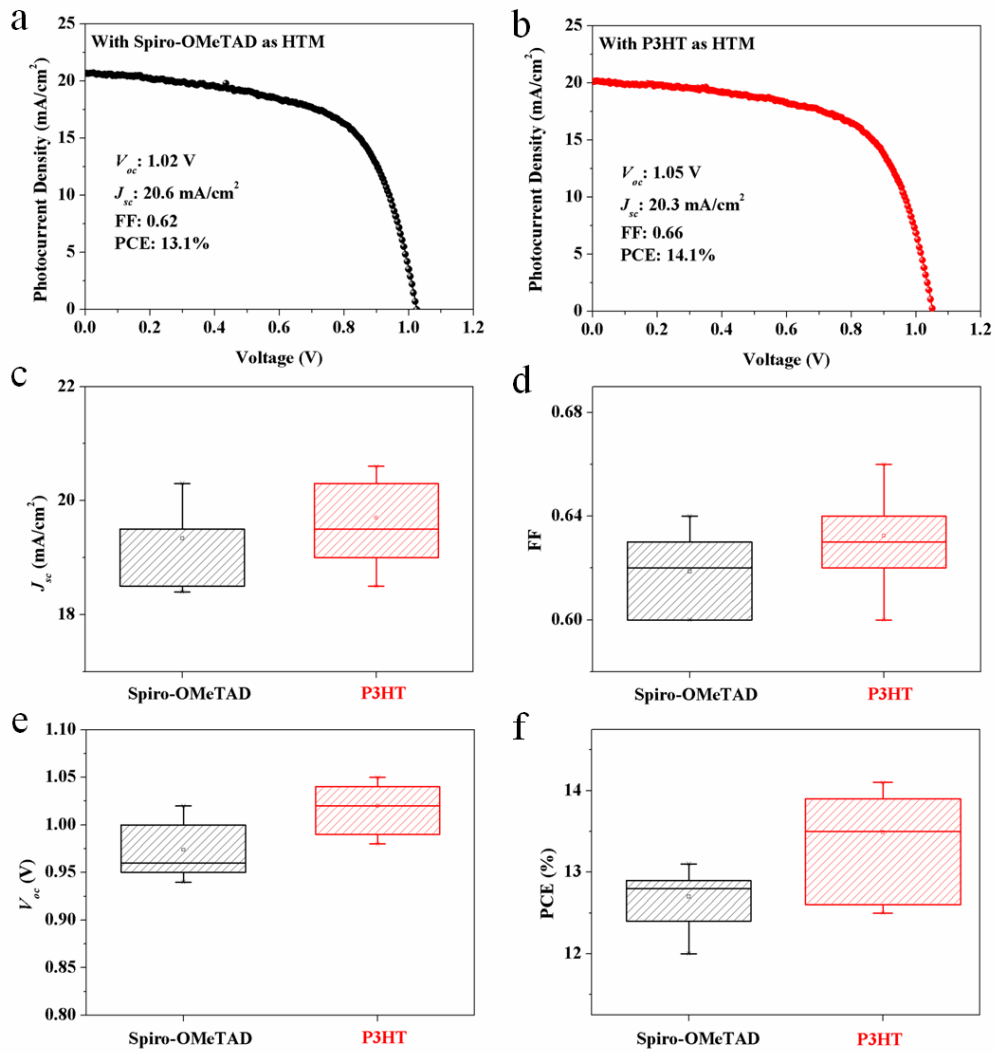


Fig. S6. J - V curve of the MAPbI₃-based PSC with (a) Spiro-OMeTAD and (b) P3HT as the HTM, which was measured under AM1.5G 100 mW/cm² illumination. Statistic of the (c) J_{sc} , (d) FF, (e) V_{oc} and (f) PCE of the MAPbI₃-based PSC with Spiro-OMeTAD and P3HT as the HTM. 12 solar cell devies from different branches were used for stastic.

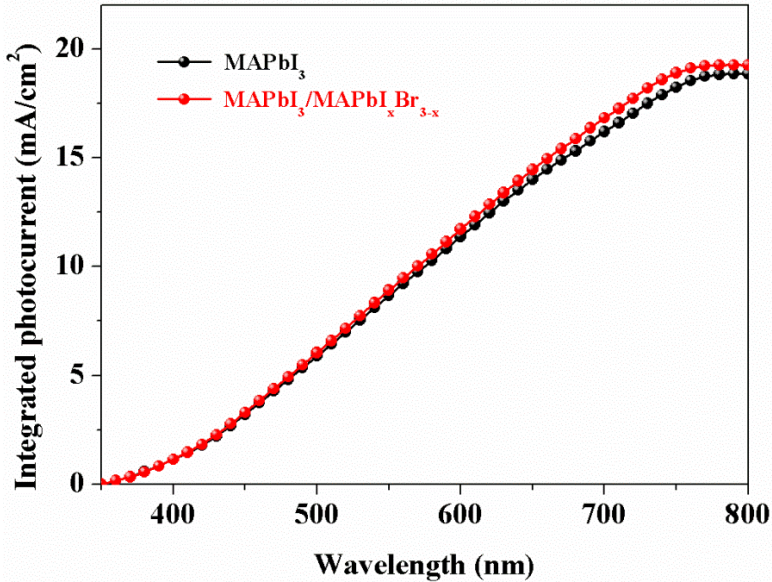


Fig. S7. Integrated photocurrent from the IPCE spectra. The photocurrent density integrated from the IPCE spectra is slightly lower than the value obtained from the *J-V* measurement, which may due to the low light intensity of the IPCE setup.

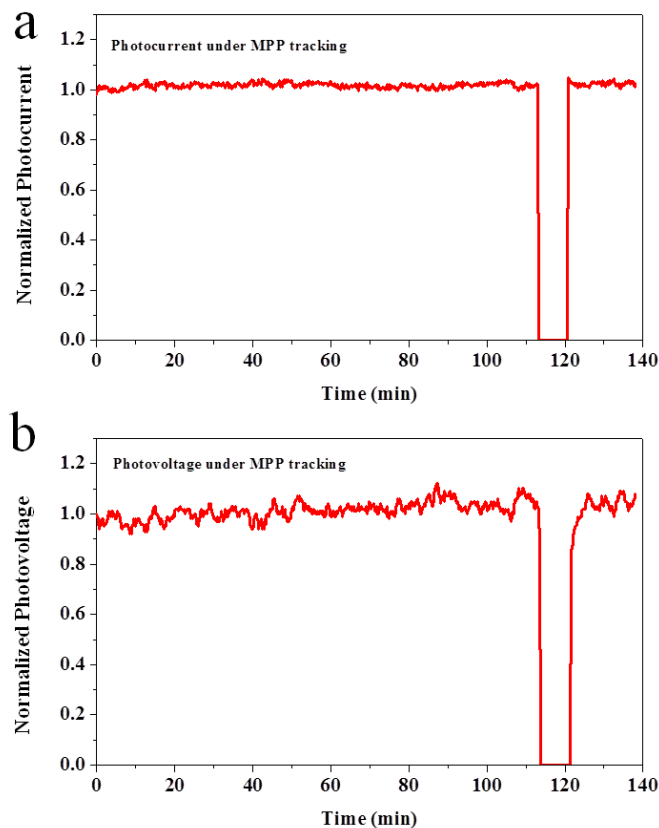


Fig. S8. MPP tracking of the (a) photocurrent density and (b) photovoltage of the $\text{MAPbI}_3/\text{MAPbI}_x\text{Br}_{3-x}$ -based PSC under continues AM1.5G 100 mW/cm² illumination.

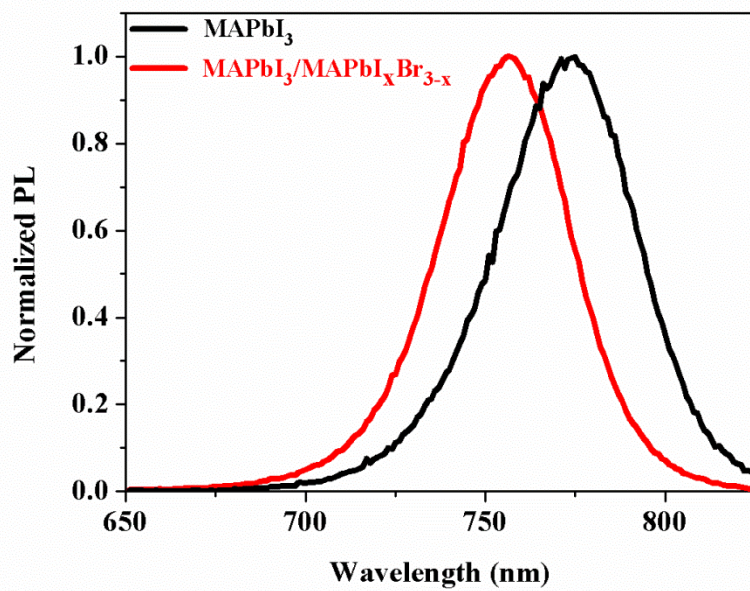


Fig. S9. Normalized PL spectra of the MAPbI_3 perovskite and $\text{MAPbI}_3/\text{MAPbI}_x\text{Br}_{3-x}$ -PSS prepared on the microscopy slide.

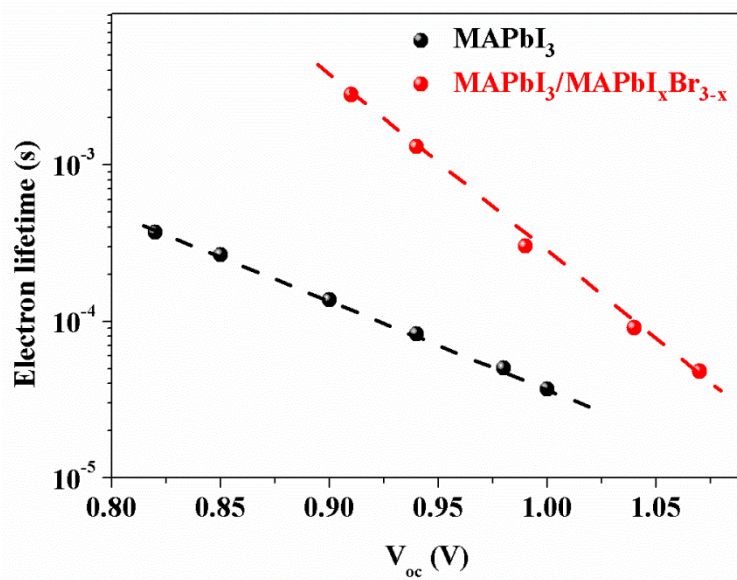


Fig. S10. Electron lifetime in the MAPbI_3 perovskite and $\text{MAPbI}_3/\text{MAPbI}_x\text{Br}_{3-x}$ -PSS solar cells as function of V_{oc} .

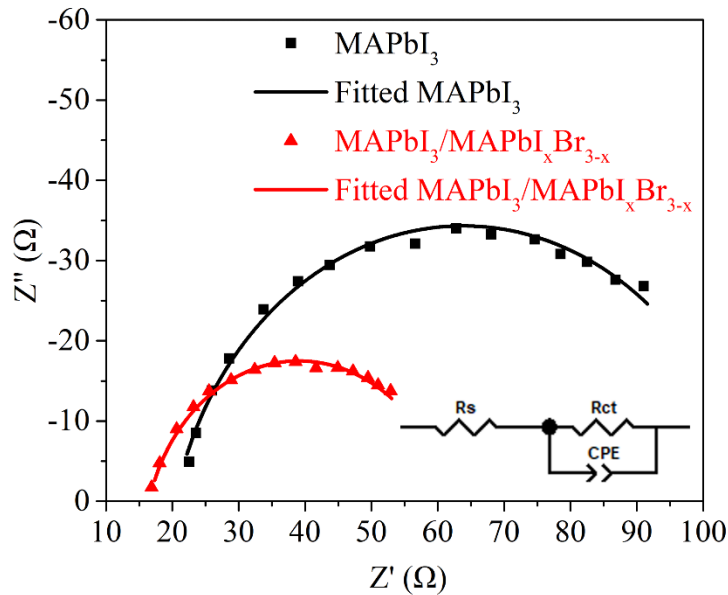


Fig. S11. Nyquist plots and their fitting curves of the MAPbI₃-based and MAPbI₃/MAPbI_xBr_{3-x}-based PSC, with the equivalent circuit depicted in the inset. In this equivalent circuit model, the high frequency arc in the Nyquist plots is attributed to the perovskite/carbon interface, which is modeled by a charge transport resistance, Rct, in parallel with a capacitance, CPE. Electrochemical impedance spectroscopy (EIS) was performed under a full-sun illumination (AM 1.5G, 100 mW/cm²) and a bias voltage of 0.8 V.

Table S1. Fitted parameters of the PL decay of the MAPbI₃-based and MAPbI₃/MAPbI_xBr_{3-x} based PSC.

Equation	$y = A_1 e^{-\frac{t}{\tau_1}} + A_2 e^{-\frac{t}{\tau_2}} + A_0$				
	A_1	τ_1 (ns)	A_2	τ_2 (ns)	A_0
MAPbI ₃	1665	2.8	193	50.8	75.4
MAPbI ₃ /MAPbI _x Br _{3-x}	1872	2.1	101	71.1	75.5

Table S2. Summarized photovoltaic performance of the carbon electrode-based HTM-free PSCs.

Device structure	V_{oc} (V)	J_{sc} (mA/cm ²)	FF	PCE (%)	Ref.
FTO/C ₆₀ /MAPbI ₃ /Carbon paste	1.07	23.44	0.613	15.38	[1]
FTO/TiO ₂ /ZrO ₂ /MAPbI ₃ /Carbon paste	0.94	23.4	0.71	15.6	[2]
FTO/TiO ₂ /MAPbI ₃ /Carbon paste	1.05	20.25	0.63	13.5	[3]
FTO/TiO ₂ /ZrO ₂ /MAPbI ₃ /Carbon paste	0.916	18.69	0.751	12.8	[4]
FTO/TiO ₂ /MAPbI ₃ /Na@C	0.78	17.94	0.64	8.89	[5]
FTO/TiO ₂ /ZrO ₂ /MAPbI ₃ /Carbon paste	0.78	21.86	0.658	11.28	[6]
FTO/TiO ₂ /ZrO ₂ /MAPbI ₃ /Carbon paste	0.94	21.45	0.77	15.6	[7]
FTO/TiO ₂ /ZrO ₂ /MAPbI ₃ /Carbon paste	0.863	21.5	0.77	14.3	[8]
FTO/TiO ₂ /ZrO ₂ /MAPbI _{3-x} (BF ₄) _x / Carbon paste	0.957	18.15	0.76	13.24	[9]
FTO/TiO ₂ /MAPbI ₃ /Bi-layer carbon paste	0.998	19.6	0.695	13.6	[10]
FTO/TiO ₂ /Al ₂ O ₃ /(5-AVA) _{0.05} (MA) _{0.95} PbI ₃ /Carbon black-graphite	0.88	21.62	0.594	11.31	[11]
FTO/TiO ₂ /Al ₂ O ₃ /MAPbI ₃ /B-MWNTs	0.92	21.50	0.77	15.23	[12]
FTO/W:TiO ₂ /MAPbI ₃ /Carbon paste	0.92	21.07	0.622	12.06	[13]
FTO/TiO ₂ /Al ₂ O ₃ /MAPbI ₃ / mesoscopic carbon	0.893	22.43	0.75	15.0	[14]
FTO/TiO ₂ /SiO ₂ /MWCNT-MAPbI ₃ / Carbon paste	0.951	22.6	62.3	12.3	[15]
FTO/TiO ₂ /MAPbI ₃ /Carbon paste	1.04	21.27	0.65	14.38	[16]
FTO/TiO ₂ /Al ₂ O ₃ /MAPbI ₃ /Carbon nanotube	0.853	17.22	0.71	10.54	[17]
FTO/TiO ₂ /Al ₂ O ₃ /MAPbI ₃ /Carbon paste	1.01	21.26	0.69	14.7	[18]
FTO/TiO ₂ /Al ₂ O ₃ /MAPbI ₃ /Carbon paste	0.846	20.04	0.723	12.3	[19]
FTO/TiO ₂ /MAPbI ₃ /Carbon paste	1.002	21.30	0.634	13.53	[20]
FTO/TiO ₂ /ZrO ₂ / (5-AVA) _x (MA) _{1-x} PbI ₃ /Carbon paste	0.858	22.8	0.66	12.84	[21]
FTO/TiO₂/MAPbI₃/MAPbI_xBr_{3-x}/ Carbon paste	1.07	20.8	0.73	16.2	This work

Table S3. Summarized photovoltaic performance of the carbon electrode-based PSCs with HTM in the device.

Device structure	V_{oc} (V)	J_{sc} (mA/cm ²)	FF	PCE (%)	Ref.
FTO/Ni(0.01):TiO ₂ / Cs _{0.05} (MA _{0.17} FA _{0.83}) _{0.95} Pb(I _{0.83} Br _{0.17}) ₃ / CuPc/Carbon paste	1.073	22.41	0.726	17.46	[22]
FTO/TiO ₂ /MAPbI ₃ /NiO-MWCNT	0.912	22.84	0.76	15.80	[23]
FTO/TiO ₂ /MAPbI ₃ /CuPc/Carbon paste	1.05	20.8	0.74	16.1	[24]
FTO/TiO ₂ /Al ₂ O ₃ / Cs _{0.05} (FA _{0.4} MA _{0.6}) _{0.95} PbI _{2.8} Br _{0.2} / NiO/Carbon paste	1.008	23.40	0.72	17.02	[25]
FTO/TiO ₂ / (FAPbI ₃) _{0.85} (MAPbBr ₃) _{0.15} / CuPc-TIPs/Carbon paste	1.01	21.4	0.65	14.0	[26]
FTO/TiO ₂ /SnO ₂ /Cs _{0.05} (MA _{0.17} FA _{0.83}) _{0.95} Pb(I _{0.83} Br _{0.17}) ₃ / CuPc/Carbon paste	0.98	23.28	0.67	15.39	[27]
FTO/TiO ₂ /ZrO ₂ /MAPbI ₃ /Co ₃ O ₄ / Carbon paste	0.88	23.43	0.64	13.27	[28]
FTO/TiO ₂ /Cs _{0.06} (MA _{0.17} FA _{0.83})Pb(I _{0.84} Br _{0.16}) ₃ /CNT s/Carbon paste	1.00	18.97	0.71	13.57	[29]
FTO/TiO ₂ /Al ₂ O ₃ /MAPbI ₃ /NiO _x / Carbon paste	0.945	17.22	0.69	12.12	[30]
FTO/TiO ₂ /ZrO ₂ /MAPbI ₃ /NiO/Carbon paste	0.97	22.38	0.50	10.83	[31]
FTO/TiO ₂ / Cs _{0.05} (MA _{0.17} FA _{0.83}) _{0.95} Pb(I _{0.83} Br _{0.17}) ₃ / Spiro-OMeTAD/SWCNT	1.12	21.0	0.71	16.1	[32]
FTO/TiO ₂ / Cs _{0.05} (MA _{0.17} FA _{0.83}) _{0.95} Pb(I _{0.83} Br _{0.17}) ₃ / Carbon cloth/Spiro-OMeTAD	1.12	20.42	0.67	15.29	[33]
FTO/TiO ₂ /ZrO ₂ /MAPbI ₃ /NiO/Carbon paste	0.917	21.36	0.76	14.9	[34]
FTO/TiO ₂ /Al ₂ O ₃ /MAPbI ₃ /NiO/ Carbon black-graphite	0.915	21.62	0.76	15.03	[35]
FTO/TiO ₂ /MAPbI ₃ /TPDI/Carbon paste	1.03	20.1	0.749	15.5	[36]
FTO/TiO ₂ /ZrO ₂ /MAPbI ₃ /NiO/Carbon paste	0.965	20.4	0.72	14.2	[37]
FTO/TiO ₂ /MAPbI ₃ /spiro-OMeTAD/CNTs	1.00	18.1	0.55	9.90	[38]
FTO/TiO ₂ /(FAPbI ₃) _{0.85} (MAPbBr ₃) _{0.15} / SWCNT:Spiro-OMeTAD	1.1	20.3	0.61	15.5	[39]

References

- [1] X. Meng, J. Zhou, J. Hou, X. Tao, S. H. Cheung, S. K. So and S. Yang, *Adv. Mater.* **2018**, *30*, 1706975.
- [2] Y. Hu, Z. Zhang, A. Mei, Y. Jiang, X. Hou, Q. Wang, K. Du, Y. Rong, Y. Zhou, G. Xu and H. Han, *Adv. Mater.* **2018**, *30*, 1705786.
- [3] Q. Q. Chu, B. Ding, Q. Qiu, Y. Liu, C.-X. Li, C.-J. Li, G.-J. Yang and B. Fang, *J. Mater. Chem. A* **2018**, *6*, 8271.
- [4] G. Huang, C. Wang, H. Zhang, S. Xu, Q. Xu and Y. Cui, *J. Mater. Chem. A* **2018**, *6*, 2449.
- [5] W. Wei and Y. H. Hu, *J. Mater. Chem. A* **2017**, *5*, 24126.
- [6] J. Baker, K. Hooper, S. Meroni, A. Pockett, J. McGettrick, Z. Wei, R. Escalante, G. Oskam, M. Carnie and T. Watson, *J. Mater. Chem. A* **2017**, *5*, 18643.
- [7] Y. Rong, X. Hou, Y. Hu, A. Mei, L. Liu, P. Wang and H. Han, *Nat. Commun.* **2017**, *8*, 14555.
- [8] S. G. Hashmi, D. Martineau, M. I. Dar, T. T. T. Myllymäki, T. Sarikka, V. Ulla, S. M. Zakeeruddin and M. Grätzel, *J. Mater. Chem. A* **2017**, *5*, 12060.
- [9] J. Chen, Y. Rong, A. Mei, Y. Xiong, T. Liu, Y. Sheng, P. Jiang, L. Hong, Y. Guan, X. Zhu, X. Hou, M. Duan, J. Zhao, X. Li and H. Han, *Adv. Energy Mater.* **2016**, *6*, 1502009.
- [10] Z. Yu, B. Chen, P. Liu, C. Wang, C. Bu, N. Cheng, S. Bai, Y. Yan and X. Zhao, *Adv. Funct. Mater.* **2016**, *26*, 4866.
- [11] F. R. Li, Y. Xu, W. Chen, S. H. Xie and J. Y. Li, *J. Mater. Chem. A* **2017**, *5*, 10374.
- [12] X. Zheng, H. Chen, Q. Li, Y. Yang, Z. Wei, Y. Bai, Y. Qiu, D. Zhou, K. S. Wong and S. Yang, *Nano Lett.* **2017**, *17*, 2496.
- [13] Y. Xiao, N. Cheng, K. K. Kondamareddy, C. Wang, P. Liu, S. Guo and X.-Z. Zhao, *J. Power Sources* **2017**, *342*, 489.
- [14] C. M. Tsai, G. W. Wu, S. Narra, H. M. Chang, N. Mohanta, H. P. Wu, C. L. Wang and E. W. G. Diau, *J. Mater. Chem. A* **2017**, *5*, 739.

- [15] N. Cheng, P. Liu, F. Qi, Y. Xiao, W. Yu, Z. Yu, W. Liu, S.-S. Guo and X.-Z. Zhao, *J. Power Sources* **2016**, *332*, 24.
- [16] H. Chen, Z. Wei, H. He, X. Zheng, K. S. Wong and S. Yang, *Adv. Energy Mater.* **2016**, *6*, 1502087.
- [17] Q. Luo, H. Ma, Y. Zhang, X. Yin, Z. Yao, N. Wang, J. Li, S. Fan, K. Jiang and H. Lin, *J. Mater. Chem. A* **2016**, *4*, 5569.
- [18] H. Li, K. Cao, J. Cui, S. Liu, X. Qiao, Y. Shen and M. Wang, *Nanoscale* **2016**, *8*, 6379.
- [19] C. Y. Chan, Y. Wang, G. W. Wu and E. Wei-Guang Diau, *J. Mater. Chem. A* **2016**, *4*, 3872.
- [20] H. Wei, J. Xiao, Y. Yang, S. Lv, J. Shi, X. Xu, J. Dong, Y. Luo, D. Li and Q. Meng, *Carbon* **2015**, *93*, 861.
- [21] A. Mei, X. Li, L. Liu, Z. Ku, T. Liu, Y. Rong, M. Xu, M. Hu, J. Chen, Y. Yang, M. Gratzel and H. Han, *Science* **2014**, *345*, 295.
- [22] X. Liu, Z. Liu, B. Sun, X. Tan, H. Ye, Y. Tu, T. Shi, Z. Tang and G. Liao, *Nano Energy* **2018**, *50*, 201.
- [23] Y. Yang, H. Chen, X. Zheng, X. Meng, T. Zhang, C. Hu, Y. Bai, S. Xiao and S. Yang, *Nano Energy* **2017**, *42*, 322.
- [24] F. Zhang, X. Yang, M. Cheng, W. Wang and L. Sun, *Nano Energy* **2016**, *20*, 108.
- [25] S. Liu, W. Huang, P. Liao, N. Pootrakulchote, H. Li, J. Lu, J. Li, F. Huang, X. Shai, X. Zhao, Y. Shen, Y.-B. Cheng and M. Wang, *J. Mater. Chem. A* **2017**, *5*, 22952.
- [26] X. Jiang, Z. Yu, H.-B. Li, Y. Zhao, J. Qu, J. Lai, W. Ma, D. Wang, X. Yang and L. Sun, *J. Mater. Chem. A* **2017**, *5*, 17862.
- [27] Z. Liu, B. Sun, X. Liu, J. Han, H. Ye, Y. Tu, C. Chen, T. Shi, Z. Tang and G. Liao, *J. Mater. Chem. A* **2018**, *6*, 7409.
- [28] A. Bashir, S. Shukla, J. H. Lew, S. Shukla, A. Bruno, D. Gupta, T. Baikie, R. Patidar, Z. Akhter, A. Priyadarshi, N. Mathews and S. G. Mhaisalkar, *Nanoscale* **2018**, *10*, 2341.

- [29] J. Ryu, K. Lee, J. Yun, H. Yu, J. Lee and J. Jang, *Small* **2017**, *13*, 1701225.
- [30] F. Behrouznejad, C.-M. Tsai, S. Narra, E. W. G. Diau and N. Taghavinia, *ACS Appl. Mater. Interfaces* **2017**, *9*, 25204.
- [31] T. A. N. Peiris, A. K. Baranwal, H. Kanda, S. Fukumoto, S. Kanaya, L. Cojocaru, T. Bessho, T. Miyasaka, H. Segawa and S. Ito, *Nanoscale* **2017**, *9*, 5475.
- [32] K. Aitola, K. Domanski, J. P. Correa-Baena, K. Sveinbjörnsson, M. Saliba, A. Abate, M. Gratzel, E. Kauppinen, E. M. J. Johansson, W. Tress, A. Hagfeldt and G. Boschloo, *Adv. Mater.* **2017**, *29*, 1606398.
- [33] S. Gholipour, J.-P. Correa-Baena, K. Domanski, T. Matsui, L. Steier, F. Giordano, F. Tajabadi, W. Tress, M. Saliba, A. Abate, A. Morteza Ali, N. Taghavinia, M. Grätzel and A. Hagfeldt, *Adv. Energy Mater.* **2016**, *6*, 1601116.
- [34] X. Xu, Z. Liu, Z. Zuo, M. Zhang, Z. Zhao, Y. Shen, H. Zhou, Q. Chen, Y. Yang and M. Wang, *Nano Lett.* **2015**, *15*, 2402.
- [35] K. Cao, Z. Zuo, J. Cui, Y. Shen, T. Moehl, S. M. Zakeeruddin, M. Grätzel and M. Wang, *Nano Energy* **2015**, *17*, 171.
- [36] F. Zhang, X. Yang, M. Cheng, J. Li, W. Wang, H. Wang and L. Sun, *J. Mater. Chem. A* **2015**, *3*, 24272.
- [37] Z. Liu, M. Zhang, X. Xu, F. Cai, H. Yuan, L. Bu, W. Li, A. Zhu, Z. Zhao, M. Wang, Y.-B. Cheng and H. He, *J. Mater. Chem. A* **2015**, *3*, 24121.
- [38] Z. Li, S. A. Kulkarni, P. P. Boix, E. Shi, A. Cao, K. Fu, S. K. Batabyal, J. Zhang, Q. Xiong, L. H. Wong, N. Mathews and S. G. Mhaisalkar, *ACS Nano* **2014**, *8*, 6797.
- [39] K. Aitola, K. Sveinbjörnsson, J.-P. Correa-Baena, A. Kaskela, A. Abate, Y. Tian, E. M. J. Johansson, M. Grätzel, E. I. Kauppinen, A. Hagfeldt and G. Boschloo, *Energy Environ. Sci.* **2016**, *9*, 461.